STREAM

IST-1999-10341

STREAM CONSORTIUM:
CNR-LAMEL / ST Microelectronics / ISEN / SOFT IMAGING SYSTEM / University of Sheffield / IMEC / CNR-IESS / University of Perugia

DELIVERABLE D17

Work package WP3

Lead participant: CNR-LAMEL

μRS measurements on test structures with different dimensions and comparison with TEM/CBED and process simulation

Main Author	Ingrid De Wolf, IMEC		
Contributing authors	Aldo Armigliato		
Date:	08-08-2001	*Doc.No:*	IST10341-IM-RP004
Keywords:	Raman, stress, 2-dimensional measurements		

Distribution list	**Project Officer:** B.Nétange (3 copies) **All Partners:** A. Armigliato LAMEL G.P. Carnevale ST Microelectronics V. Senez ISEN T. Schilling Soft Imaging System A.G.Cullis USFD (University of Sheffield) I. De Wolf IMEC S. Lagomarsino CNR-IESS G. Carlotti UniPg (University of Perugia)

Table of contents

1. Experimental set-up and samples 4
   1.1 Raman spectroscopy experiments 4
   1.2 Samples and structures 6
      1.2.1 Samples 6
      1.2.2 Structures 6
2. Results from the first measurement campaign 7
3. Results from the second measurement campaign 9
4. Raman experiments on a cross-section TEM-sample (V004808_20) 9
      4.1.1 TEM-sample 9
      4.1.2 Line scan 11
      4.1.3 Two-dimensional scan. 17
5. Comparison with analytical models 27
6. Comparison with numerical models 28
7. Comparison with CBED 28
8. General conclusions 28
References 29

Abstract

This deliverable discusses the micro-Raman spectroscopy (µRS) results obtained on different wafers and on structures with different dimensions. Both one-dimensional Raman scans performed on top of the samples and two-dimensional scans performed on the cross-section of samples (TEM samples) are discussed.

Some of these results were already reported in the intermediate reports IST10341-IM-RP002 (samples from first measurement campaign) and IST10341-IM-RP003 (samples from second measurement campaign). They are briefly summarised in this report, the reader is referred to the reports for more detailed information. Only new, not yet reported data are discussed in more detail. The report also discusses the comparison of the results with data from CBED and with simulations. Also this comparison was already mostly discussed in some previous reports and deliverables (IST10341-IS-RP004 (D12a)) and D8 (IST10341-LA-RP005).

.

1. Experimental set-up and samples

1.1 Raman spectroscopy experiments

Most Raman experiments were performed using the 457.9 nm line of an Argon laser. The light was focused on the sample using a 100x objective lens. The sample was positioned under the microscope on an XY-stage and moved in small steps of 0.1 µm or larger. At each position a Raman spectrum was measured. The autofocus system was used to obtain a similar focusing for all structures. See also IST10341-IM-RP001.
Some experiments on samples from campaign 2 were performed using the 514 nm laser line.
In some experiments the oil immersion objective was used in order to have a better spatial resolution (see IST10341-IM-RP001). However, due to problems with the oil (burning), it was decided that most experiments should be done using the normal 100x objective lens.
One of the most interesting characteristics of the Raman spectrum is its sensitivity for strain in the sample. When the material is under strain, this may cause a shift of the frequency of the Raman signal. To calculate the relation between Raman shift and strain, one has to solve the "secular equation". For diamond-type (O_h point group) or zinc-blende type (T_d point group) semiconductors this is given by [1,2]:

$$\begin{vmatrix} p\varepsilon_{11}+q(\varepsilon_{22}+\varepsilon_{33})-\lambda & 2r\varepsilon_{12} & 2r\varepsilon_{13} \\ 2r\varepsilon_{12} & p\varepsilon_{22}+q(\varepsilon_{33}+\varepsilon_{11})-\lambda & 2r\varepsilon_{23} \\ 2r\varepsilon_{13} & 2r\varepsilon_{23} & p\varepsilon_{33}+q(\varepsilon_{11}+\varepsilon_{22})-\lambda \end{vmatrix} = 0 \qquad (1.1)$$

where ε_{ij} are the strain tensor elements and p, q, r are the so called phonon material constants.
If the frequency of the Raman signal under study is ω, and the stress-free value is ω_o, then the strain induced shift of the Raman frequency, $\Delta\omega$, is given by:

$$\Delta\omega = \omega - \omega_o \approx \frac{\lambda}{2\omega_0} = f(\varepsilon_{ij}) \qquad (1.2)$$

It is in general impossible to solve the secular equation (Eq. 1.1) if the strain tensor components are not known. So, certain assumptions about the stress or strain distribution in the sample are required,

or data from CBED or from numerical analysis have to be used. For example, for uniaxial or biaxial stress, one obtains a linear relation between stress and Raman shift [3]. For silicon this is given by [4]:

$$\sigma \text{ (MPa)} \approx -434 \times \Delta\omega \text{ (cm}^{-1}\text{)} \qquad (1.3)$$

This equation shows that a positive shift of the Raman peak, $\Delta\omega > 0$, indicates compressive stress, while a negative shift, $\Delta\omega < 0$, indicates tensile stress.

In order to determine the Raman frequency for strain measurements, the measured Raman peak is fitted with a Lorentz function. The plasma lines of the laser are used as reference. They are fitted using a Gauss function to determine their frequency. Variations in the position of the plasma line are due to instrumental variations (laser, room temperature…). The Raman spectra are corrected for these variations.

Fig. 1.1 shows a typical spectrum as obtained in one point on a Si sample. For all measurement points, the measured Si Raman peak is fitted with a Lorentz function to estimate its frequency, full width at half maximum, and intensity. In addition, the spectra were fitted with an asymmetrical Lorentz function to monitor the degree of asymmetry of the Raman peaks.

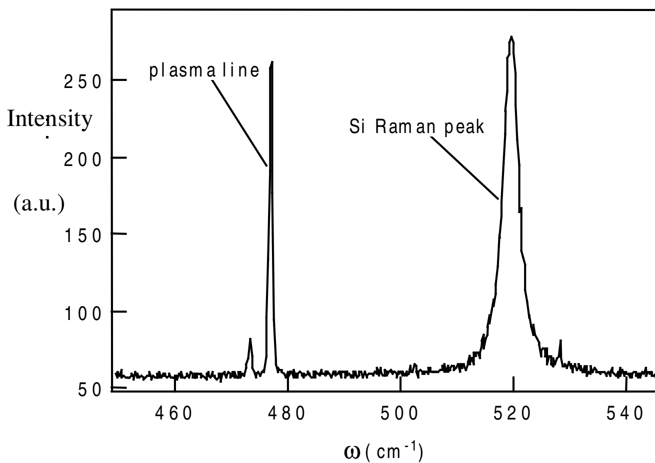

Figure 1.1 - *Raman spectrum of crystalline silicon, measured using the 457.8 nm laser line. It shows the Si Raman peak and plasma lines from the laser.*

In addition to the Si Raman peak, also plasma lines from the laser were fitted, using a Gauss function. These were used for calibration purposes.

1.2 Samples and structures

1.2.1 Samples

- The samples used for the first Raman spectroscopy measurement campaign are listed in Table I (see Deliverable D1, IST10341-ST-RP001). From each sample, two chips were obtained.

Table I: *Samples*

Sample Code	Nitride (nm)	HDP1 + TEOS	HDP1 + HDP2	Oxide anneal
V004808_1	160	«		
V004808_2	160	«		«
V004808_7	160		«	
V004808_8	160		«	«
V004808_13	120	«		
V004808_14	120	«		«
V004808_19	120		«	
V004808_20	120		«	«

- The samples used from for the second Raman spectroscopy measurement campaign are listed in Table II.

Table II: *Samples from the second campaign*

Sample Code	STI	Oxide mask	Wafer nr	salicide
A044733	«		**10**	300Å Ti/250Å TiN
	«		**14**	300Å Ti/150Å TiN
	«		**18**	300Å Ti
	«		**22**	400Å Ti
A046324		«	**3**	300Å Ti/250Å TiN
		«	**7**	300Å Ti/150Å TiN
		«	**11**	300Å Ti
		«	**14**	400Å Ti

- A sample used for TEM analysis was provided by LAMEL for Raman experiments on the cross-section of the sample. This sample was made from chip V004808_20, structure 5.

1.2.2 Structures

Three different kinds of structures were measured for all samples (see Fig. 1.2): structure 11 (see IST10341-ST-PR001, pg. 16) a1=2.0, s1=4.2, a2=25, s2=3.5, a3=25, s3=4.2,… (in µm, a=active, s=space), structure A and structure B. In addition on some samples structure 5 and some smaller structures where measured. Structure 5 is similar to structure 11, the only difference is that it has a spacing of 6 µm instead of 4.2 µm.

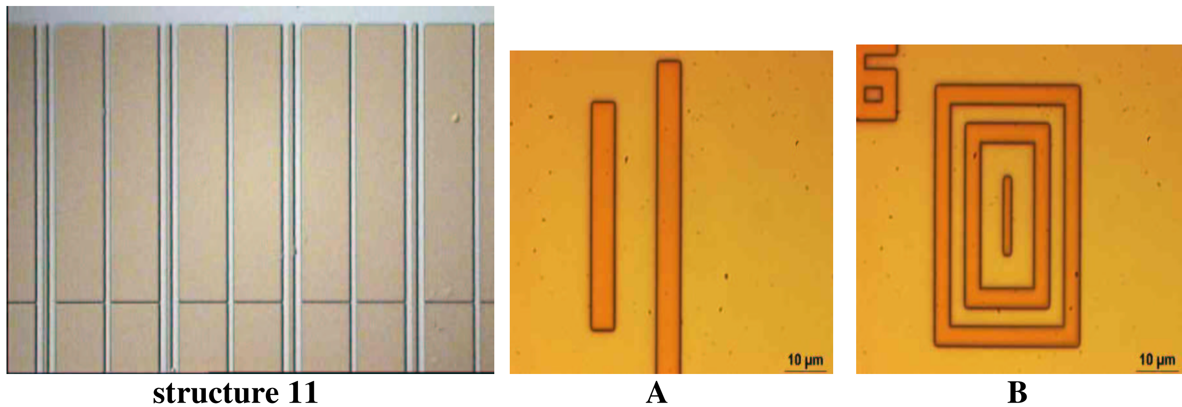

Figure 1.2: *Photograph of structure 11, A and B*

2. Results from the first measurement campaign

The results from the first measurement campaign were discussed in the intermediate report IST10341-IM-RP002.

Figure 2.1 shows a typical result of a Raman experiment on structure 11 (sample V00484_20). The shift of the Raman frequency from the stress free value, $\Delta\omega$, is plotted as a function of the position on the sample. This shift is related to the stress in the sample: $\Delta\omega > 0$ indicates compressive stress, $\Delta\omega < 0$ indicates tensile stress.

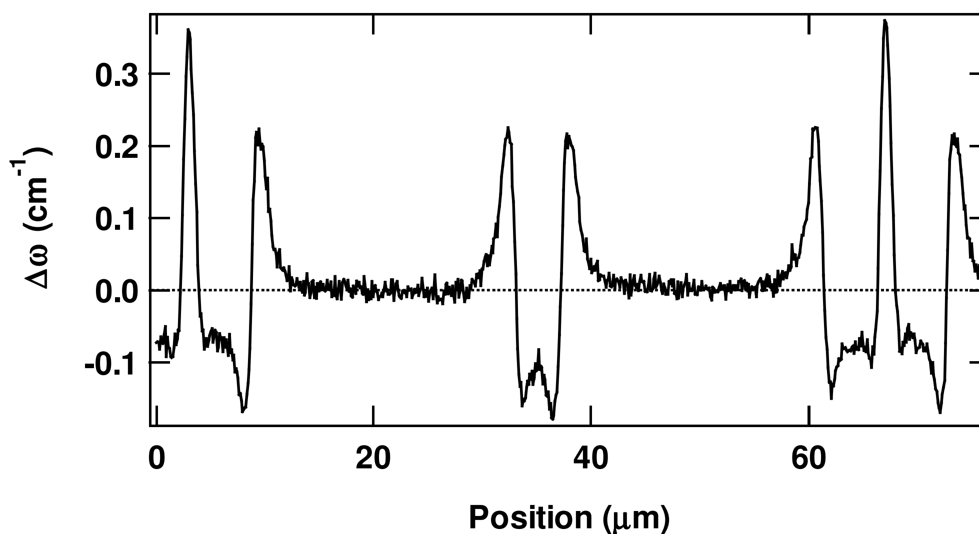

Figure 2.1: *Raman experiment result on sample V00484_20, structure 11.*

The main conclusions were:

- There is compressive stress at the edges of the active region
- This compressive stress relaxes towards the center of the active region and becomes zero at about 5.5 µm from the edge. From this it can be expected that for active regions smaller than 11 µm, the stress will not become zero anymore in the center.

- There is tensile stress just outside the edges: this is either at the side wall of the active region or at the trench bottom. The exact location can not be distinguished with Raman due to the limited spatial resolution.
- The narrower the active region, the larger the compressive stress within that region.
- At least part of the stress measured in the active area comes from the nitride. This stress increases with increasing nitride thickness.
- Stress induced by HDP1+TEOS is slightly larger than the stress induced by HDP1+HDP2. However, the difference is very small.
- Oxide anneal results in a decrease of the compressive stress in samples with HDP1+TEOS and in a slight increase of the compressive stress in samples with HDP1+HDP2.

The stress in structure 11 of sample V00484_14 was found to be much smaller than in the other samples, compare for example figure 2.2 (V00484_14) with figure 2.1 (V00484_20). It also did not fit with the numerical simulations (see report IST10341-IS-RP004, pg. 23, Fig. 21b). In order to check whether this was a measurement error, a new Raman experiment was performed on this sample. The result is shown in Fig. 2.3. The stress measured in this case is indeed higher than measured before. A third measurement (not shown) confirmed these results. The results indicate that there was a problem with the focus in the first measurement shown in Fig. 2.2.

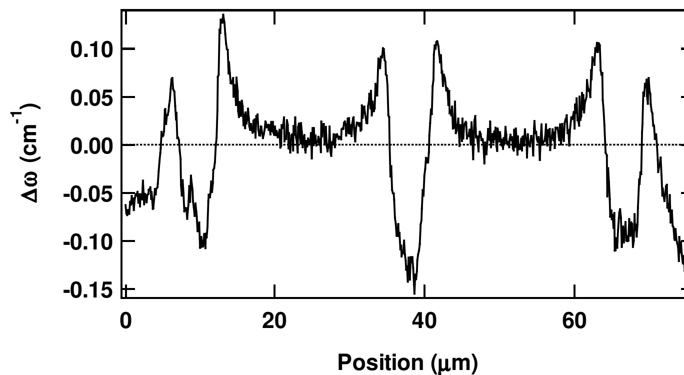

Figure 2.2: *Raman experiment result on sample V00484_14, structure 11.*

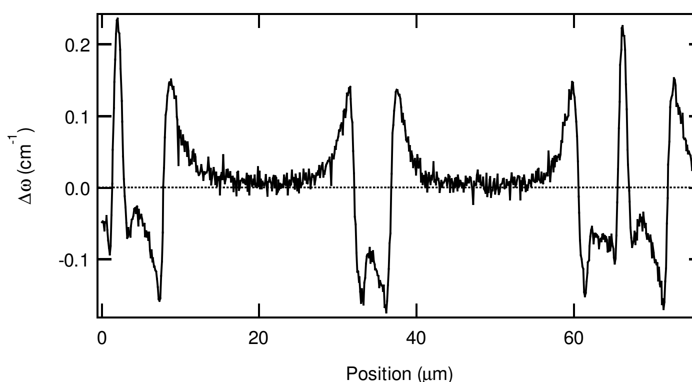

Figure 2.3: *Second Raman experiment result on sample V00484_14, structure 11.*

According to the simulations, the maximal positive Raman shift in the 2 μm active area should be about 0.25 cm^{-1}. This fits very well with what we observe in the new experiment (Fig. 2.3).

3. Results from the second measurement campaign

The results from the second measurement campaign were discussed in the intermediate report IST10341-IM-RP003.
These samples had a silicide layer on top of the active area. It was found that they were not transparent for the laser light used in these Raman experiments. This means that we could not obtain a signal from underneath these structures and study the stress. We could only compare samples indirectly, through looking at the stress at the left and right side of the lines.

The following conclusions could be drawn from these experiments:
In between the silicide lines we observe:

- no difference in stress between the 300Å Ti/250Å TiN sample and the 300Å Ti/150Å TiN sample
- a larger stress in the sample with thicker $TiSi_2$ silicide
- an increase of the tensile stress with decreasing line width

Because of the mask inversion, we could not compare stress in batch A044733 and A046324. It will be looked into whether a comparison can be made on another structure of the sample.

4. Raman experiments on a cross-section TEM-sample (V004808_20)

It was decided that Raman spectroscopy experiments should be performed on cross-sections of samples. This because of two reasons:

- From the comparison of Raman spectroscopy data with CBED data, it was concluded that a direct comparison is very difficult because Raman data are obtained from the top side of the sample and do not give a value of the strain at one certain position (a certain width and depth) in the sample as CBED does, but a weighted value of the stress in depth at a certain width position.
- For the validation of CBED results and models, it is important to find out how whether thinning of a sample for CBED measurements would result in stress relaxation.

4.1.1 TEM-sample

A TEM prepared sample (V004808_20, prepared for structure 5) was obtained from LAMEL.
Structure 5 is depicted in Fig. 4.1 (see IST10341-ST-RP001, pg. 16) and a top view is shown in Fig. 4.2. The dimensions are: a1=2.0, s1=6, a2=25, s2=3.5, a3=25, s3=6,… (a=active, s=space)

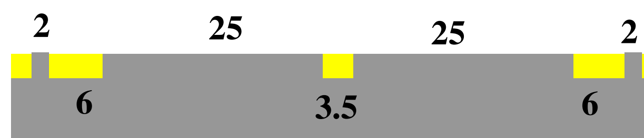

Figure 4.1: *Cross section of structure 5. The widths are indicated in um. Yellow: trench, grey: silicon.*

Figure 4.2: *Photograph of region 5, taken on top of chip (not TEM sample).Blue: trenches, brown: active.*

This structure has two typical features: a 2 µm active region isolated by 6 µm wide trenches, and a 3.5 µm trench isolated by 25 µm wide active regions.
Figure 4.3 shows a photograph of the TEM-sample taken with a microscope. The sample consists of two Si pieces glued together (to avid damage during sample preparation). One clearly sees the hole next to which the sample is very thin. Figure 4.4 zooms in on the area where the measurements will be performed. The 2 µm wide active area isolated by 6 µm wide trenches of structure 5 (see inset figure 4.4) can be distinguished at three positions on the sample, close to the hole in the sample, where the sample is thinnest (position 1), further away (position 2) and still further away (position 3).

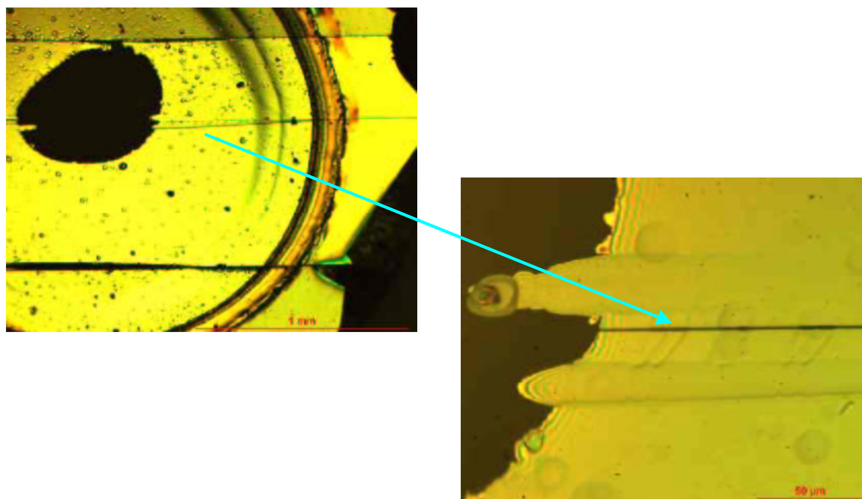

Figure 4.3: *Photograph of the TEM sample (left) and zoom in on right side (right).*

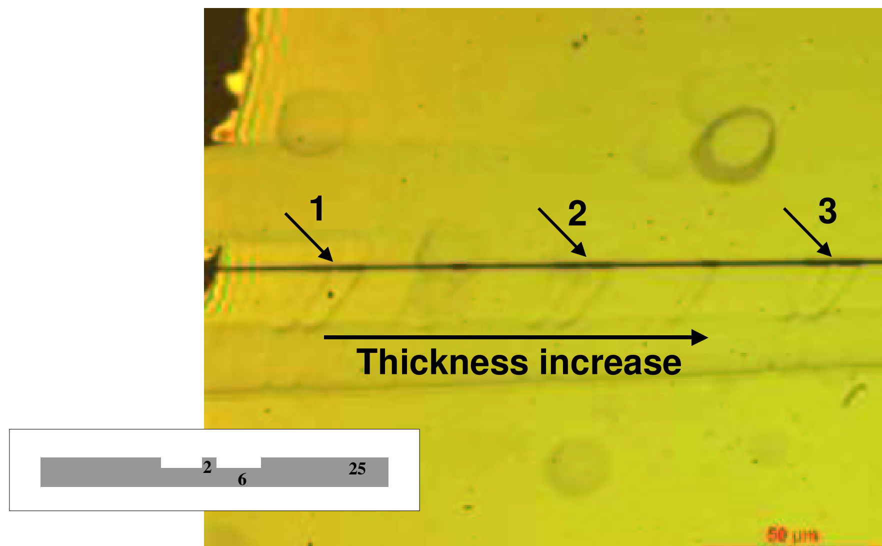

Figure 4.4: *Photograph of the TEM sample where the Raman measurements are performed. The 2 μm active regions which are measured by Raman are indicated (regions 1, 2 and 3). Inset: dimensions and topology of the three regions.*

4.1.2 Line scan

Before starting two-dimensional measurements, a line scan was performed starting at the hole, and scanning across structures 1, 2 and 3. This scan was done as close as possible to the surface of the wafer, so that stress induced by the trenches in the silicon could be measured. It is impossible to know the 'exact' location of the focused laser spot on the sample, i.e. whether the center of the spot is exactly at the surface of the active areas, or at the surface of the trenches, or lower or higher, because the 100x magnification of the Raman instrument does not allow such an exact positioning.
The first two attempts (each taking about 1 day of measurement time) to perform this experiment failed due to problems with the detector of the Raman instrument, defocusing during the experiment, and not completely correct positioning (it takes a lot of skill and patience and some luck to position the sample on the XY-stage of the microscope in such a way that a 1 μm laser spot stays at the same distance from the surface of the sample during a scan across 200 μm). The third measurement turned out very well and is discussed in the following.
The measurement started at the side of the hole. The focus of the laser was controlled regularly during the entire experiment. The output power of the laser was 5 mW, which corresponds with a power on the sample of about 1.5 mW (concentrated in the focused laser beam).
Figures 4.5 shows the Raman intensity measured during this line scan on the cross-section TEM sample, close to the wafer surface. The intensity shows some local variations near the structures, but its baseline level stays, far from the edge of the hole, rather constant at about 700 a.u.. The local variations indicate that the focused laser spot is located at a position where it probes at least part of the trench oxide. If it would be located lower, we would not see these variations. They indicate the position of the active areas. At the start of the experiment, near the hole, the intensity is very small and increases with distance from the hole.

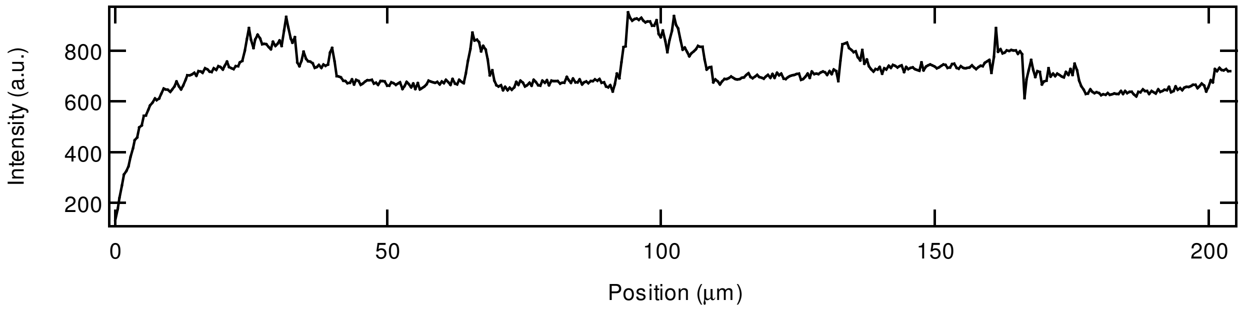

Figure 4.5: *Raman intensity as a function of distance from the hole in the TEM sample. Measurement along on the cross-section of the sample close to the wafer surface.*

This can be explained by an increase of thickness of the sample until the sample thickness is larger than the penetration depth d_p of the laser light, as shown in Fig. 4.6. As long as the sample thickness is smaller than the penetration depth of the laser light in the sample, the Raman intensity will increase with distance x. As soon as $x > x_p$, i.e. when the thickness of the sample is larger than the penetration depth of the light, the intensity will remain constant. The penetration depth of Raman is mostly defined as the depth where the Raman intensity drops to 10% of it's maximal value. This is made more clear in the following.

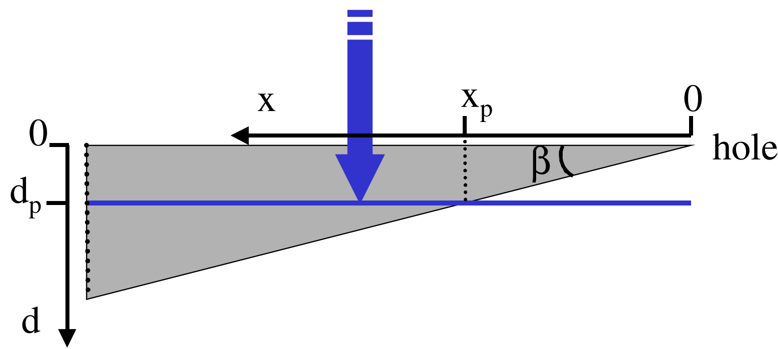

Figure 4.6: *Drawing indicating the relation between depth d_p of Raman signal, distance x from the hole in the sample and angle β of the sample.*

From the change of the intensity with distance x from the hole, it must be possible to calculate the thickness of the sample. Consider the following equations:
The total Raman scattered light intensity I_{total}, can be splitted into two parts, I_S and I_d. I_S is the part coming from the surface to a certain depth d:

$$I_S = I_o D \int_0^d e^{-2\alpha d} dx = \frac{I_o D}{2\alpha}(1 - e^{-2\alpha d}) \qquad (4.1)$$

where I_o, D and α are the incident light intensity, the Raman scattering cross section and the photo-absorption coefficient of silicon, respectively. The factor '2' arises because the light has to go in and out of the material to be detected.
And I_d is the Raman scattered light intensity integrated from the depth d to infinity is given by

$$I_d = I_o D \int_d^{\infty} e^{-2\alpha d} dx = \frac{I_o D}{2\alpha} e^{-2\alpha d} \tag{4.2}$$

For the 457.9 nm wavelength of Si, $\alpha = 3.666\ 10^6\ m^{-1}$ [5]
The penetration depth of Raman, d_p, is defined as the depth where 90% of the total Raman intensity comes from. I.e., I_d constitutes of only 10% of the total intensity ($I_{total} = I_S + I_d$), or

$$\frac{I_d}{I_S + I_d} = 0.1 \tag{4.3}$$

this is for a depth

$$d_p = -\ln(0.1)/2\alpha \tag{4.4}$$

for Si and a laser light wavelength of 457.9 nm, this is $d_p = 313$ nm [5].

If we assume that the shape of the sample is a sharp triangle with angle β (see Fig. 4.6), then the relation between the thickness 'd' of the sample and the distance 'x' from the edge is given by

$$d = tg(\beta)\ x \tag{4.2}$$

and Eq. 4.1 becomes

$$I_S(x) = \frac{I_o D}{2\alpha}(1 - e^{-2\alpha . tg(\beta) . x}) \tag{4.3}$$

Figure 4.7 (red curve) shows a fit of an exponential relation to the part of the Raman intensity curve where the intensity changes (so for $x < x_p$), close to the hole. As can be seen in this figure, a very good fit is obtained, giving a value for $tg(\beta) = 0.0270 \pm 0.0006$ or $\beta = 1.54^o \pm 0.03^o$. From this fit, we know the relation between sample thickness and position (Eq. 4.2).

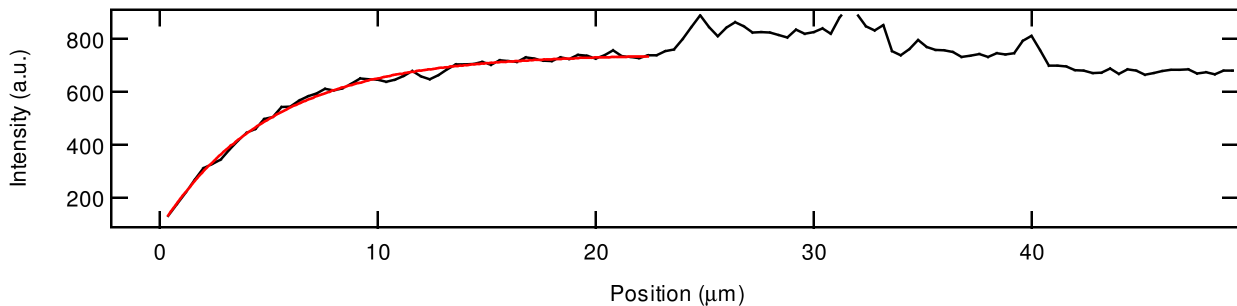

Figure 4.7: *Black curve: measured change of the Raman intensity as a distance from the hole in the TEM sample. Red curve: Fit of Equation 3 to the Raman intensity as a function of the position.*

The maximal intensity given by the fit is 740.6 a.u. According to the above definition of penetration depth, we can assume that this depth is reached when the additional intensity variation is smaller than 10%, i.e. at a sample thickness where the intensity is 740.63 – 74.063 = 666.57. This is at a thickness of 0.297 µm. So, from the experiment follows that d_p is about 300 nm.

Figure 4.8 shows the variation of the Raman peak position (Raman frequency, ω) with distance from the hole in the TEM sample. On top of the figure, a schematic drawing is shown indicating the position of the trenches. We clearly see two kinds of variation of ω:

- a local variation of ω near the STI structures: this is due to the local stress variation near the structures
- an overall decrease of ω towards the hole in the sample (position 0): this is not due to a stress variation, but mostly to a change in the local temperature of the sample

We will discuss these results in the following.
The red line in the figure indicates the thickness variation of the sample, obtained from the above discussed fit.

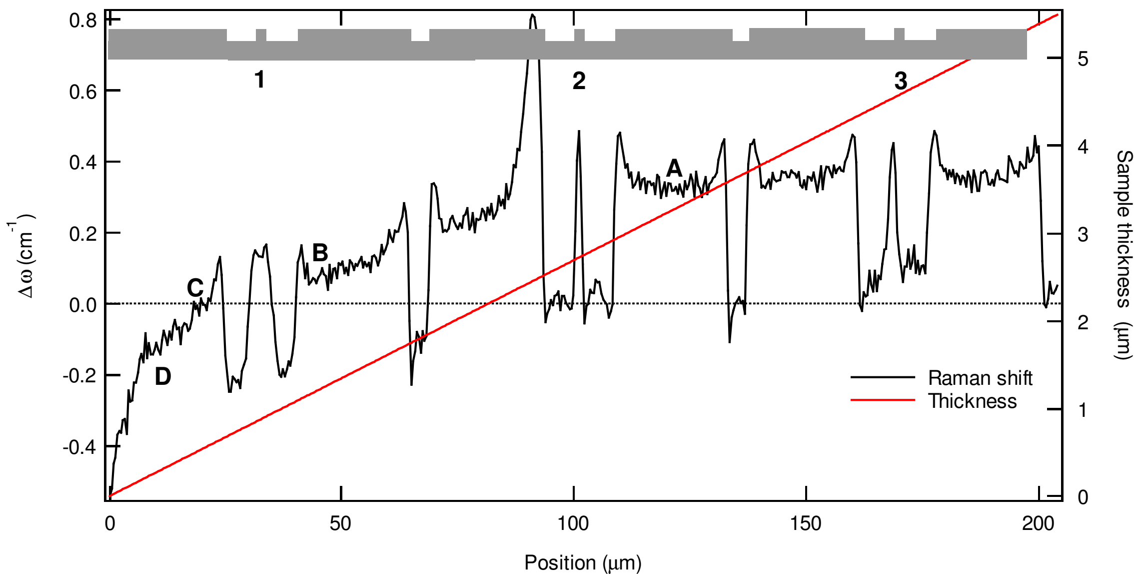

Figure 4.8: *Black curve: Raman frequency shift as a function of distance from the hole in the TEM sample. Measurement along the top surface on the cross-section of the sample. Red curve: thickness variation of the sample as calculated from the variation of the Raman intensity and Eq. 1-3.*

It is well known that the laser light, focused on the sample to a spot size of about 1 µm, induces some local heating of the sample. As long as the thickness of the sample is constant, this heating is the same on all places of the sample. However, for thin or small samples, the heat can not easily flow away in the sample and the local heating will be larger. The Raman frequency is dependent on the temperature, local heating will induce a downshift of the signal. The relation between temperature variation T and Raman peak position of silicon is given by [5]:

$$\Delta\omega = -0.0242\ \Delta T \qquad (4.4)$$

So, the decrease of the Raman frequency close to the hole in the TEM sample is most likely predominantly due to local heating because of the thin sample, i.e. due to a temperature increase. This phenomenon was observed and studied at IMEC in the past, in MEMS structures (narrow long beams and thin membranes) [6], and on oxide lines for the EC project Nostradamus [7]. That this heating effect occurs is also confirmed by the 2-dim Raman experiments (see further on). The decrease of the frequency, i.e. the onset of the heating, starts at a distance of about 85 to 95 µm from the hole, this corresponds with a sample thickness of about 2.3 to 2.6 µm.
In figure 4.8 four points, A, B, C and D are indicated. We assume that the stress in these points is the same, so we assume that there is no stress relaxation due to sample thinning. So, the change in

$\Delta\omega$ between these points is due to a change in local heating because of sample thinning. Assume that at point A ($\Delta\omega_A$ = 0.328 cm^{-1}) there is no heating effect yet (sample thick enough to dissipate heat). We take that point as reference. Just before structure 1, point B ($\Delta\omega_B$ = 0.083 cm^{-1}) is shifted down with respect to A with $\Delta\omega_A - \Delta\omega_B$ = 0.328 – 0.083 = 0.245 cm^{-1}. This corresponds with a temperature increase of ΔT = 10 ^{o}C. Point C ($\Delta\omega_C$ = -0.003 cm^{-1}) is shifted down with respect to A with $\Delta\omega_A - \Delta\omega_C$ = 0.331 cm^{-1}, indicating a temperature increase of 13.7 ^{o}C. So, if this overall downshift is only due to a temperature change in the sample, then the temperature induced by the laser beam in structure 1 is about 12 ^{o}C higher than in structure 2 or 3. The latter two are about at the same temperature. Close to the hole, $\Delta\omega$ = -0.54 cm^{-1}, indicating a temperature increase with 36°C (if this downshift is entirely due to temperature). CBED measurements are typically performed at positions where the silicon is even thinner than the position of structure 1, i.e. where the thickness is 0.3 µm. At that position (see D in Fig. 4.8) the shift is about $\Delta\omega_D$ = -0.143 cm^{-1}, a difference with point A of 0.471 cm^{-1}, corresponding with a temperature increase of 19.5 ^{o}C.

So, from these experiments it is clear that some local heating is induced by the Raman probing beam in the TEM sample. This heating increases with decreasing sample thickness when this thickness is smaller than about 2.6 µm. As a result, structure 1 has during the Raman measurement a (local) temperature which is about 12 ^{o}C higher than structure 2 and 3.

We corrected for this temperature induced variation by subtracting the slowly changing background from the total Raman shift curve. The result is shown in Figure 4.9.

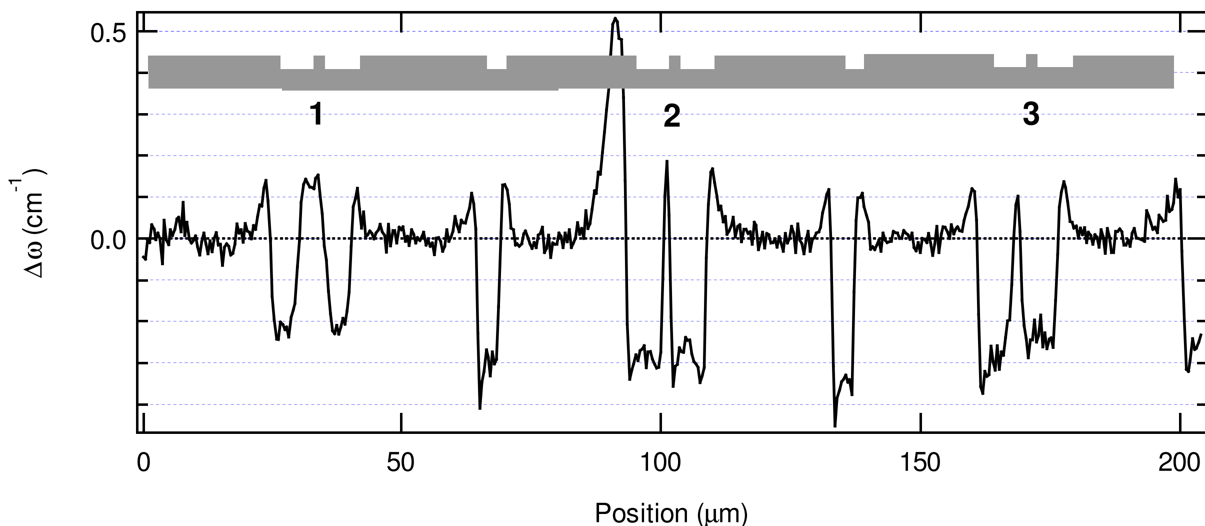

Figure 4.9: *Raman frequency shift as a function of distance from the hole in the TEM sample, after correction for heating effects. Measurement along the top surface on the cross-section of the sample.*

We assumed that the stress in between the structures is zero. This assumption is not necessary correct.

Fig. 4.9 shows a similar variation in stress near structures 3 and 2. However, near structure 1, the stress seems to be less tensile and to have a broader distribution in the active region. *This effect might be due to two reasons: stress relaxation due to sample preparation, and/or stress affected by local heating with the laser beam.*

There is a strange local increase in stress near structure 2. This is probably due to some local damage to the sample during sample preparation.

Figure 4.10 compares the Raman data measured on the cross section of sample 20 (black, on structure 2 and 3 (no heating)) with the data measured from the top on a similar sample (red, chip, no TEM sample). If we assume the stress in between the structures to be the same, we clearly see a difference. The difference between maximum and minimum stress in the 2 µm isolated structures seems to be about the same, but the overall Raman signal is shifted to higher frequencies in the measurement from the top surface. One has to take into account that the measurements from the top were done along a (100) axis direction, while the measurements from the side were along a (110) direction. I.e. probably another Raman phonon is observed when measuring from the side (a TO phonon) than when measuring from the top, and the relation between stress and phonon shift might be different. First calculations were performed assuming that the shear stress is zero (otherwise the calculations become very complicated). They showed that the relation between Raman shift and stress along the width (σ_{xx}) and depth (σ_{zz}) of the STI active regions is indeed different when measuring from the top of the sample and from a cross section (the probing laser light is along a [100] crystal axis in the first case, and along [110] in the second case). We obtained the following relation:

Probing from top (100) surface :

$$\Delta\omega = -1.93 \text{ E-9 } \sigma_{xx} - 0.75 \text{ E-9 } \sigma_{zz}$$

Probing on cleaved (110) surface:

$$\Delta\omega = -0.365 \text{ E-9 } \sigma_{xx} - 2.31 \text{ E-9 } \sigma_{zz}$$

These calculations still have to be checked, but if they are correct, this means that when probing from the top surface, the Raman shift is mostly affected by the stress along the width of the structures, σ_{xx}. And when probing along the cross section, the Raman shift is mainly determined by the stress along the depth (σ_{zz}). If we can neglect the shear stress, we could calculate the different stress components along x and z direction from this experiment and compare this with numerical simulations. This work is in progress.

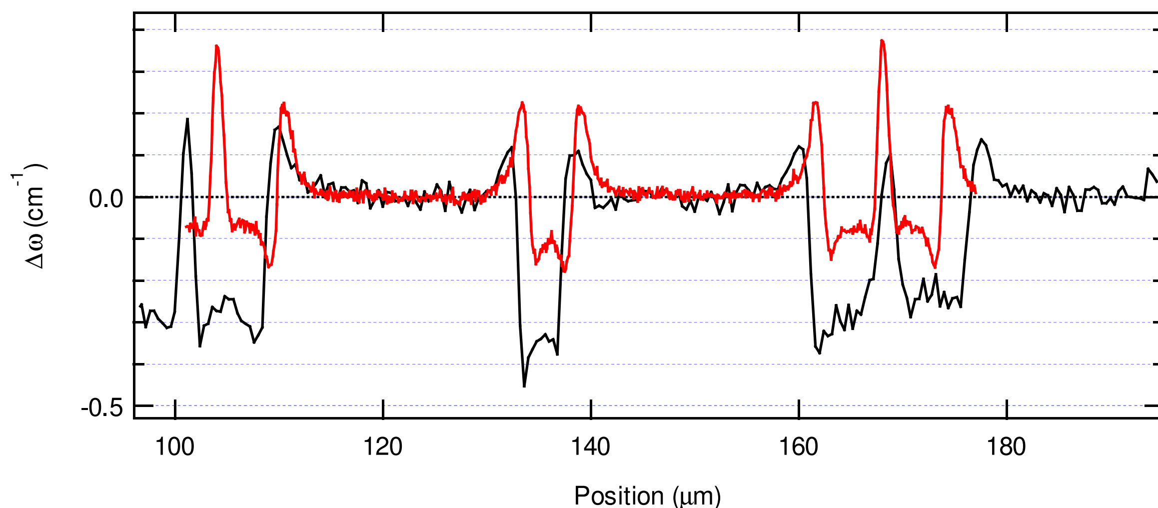

Figure 4.10: *Black curve: Raman frequency shift measured on the TEM sample in cross-section, near structure 2 and 3 (see Fig. 4.4-4.9, after correction for heating effects). Measurement close to the wafer surface on the cross-section of the sample. Red curve: Measurement on similar structures from the top surface of the sample (on a not-cross-sectioned thinned sample, i.e. a bulk chip).*

4.1.3 Two-dimensional scan.

Two-dimensional Raman experiments were performed on the 2 µm active region of structure 1, 2 and 3 of Figure 4.4. Figure 4.11 shows the position of the square region which was probed on structure number 3. A region of x = 10.4 µm by z = 8.8 µm was probed. The step size was 0.2 µm and the integration time/point was 25 sec. This counted to a total number of measured data points (Raman spectra) of 2288, and a measurement time of 16.5 hours. The additional fitting and correcting of the data took at least one additional day. We performed two of such measurements on structure 1, 2 and 3, each, so in total 6 measurements. The results are discussed in the following, starting with structure 3.

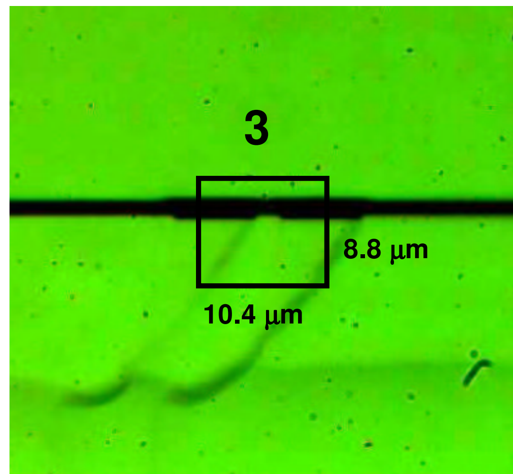

Figure 4.11: *Position of two-dimensional Raman experiment: square region probed on structure number 3.*

4.1.3.1 Structure 3

We started the experiments on structure 3, because this structure was located far away from the hole, at a position where the sample was thick enough so that it could be assumed to have no influence on the measured stress due to stress relaxation or heating.

Figure 4.12 shows the measured intensity for the two experiments performed on this structure. The x (position) and y (depth)-axes are in µm. One can clearly distinguish the structure: we find a larger intensity at the active region (blue) and a lower intensity (red) at the position of the 6 µm wide trenches. The measured region is slightly shifted right in the first experiment, compared with the region we intended to measure (see Fig. 4.11). Also in experiment 2, the measured region was shifted, the blue line at the left indicates the 2 µm structure, the 6 µm wide trench is in the center (see drawing at the top). This is due to an instrumentation error in the Raman instrument and is difficult to avoid.

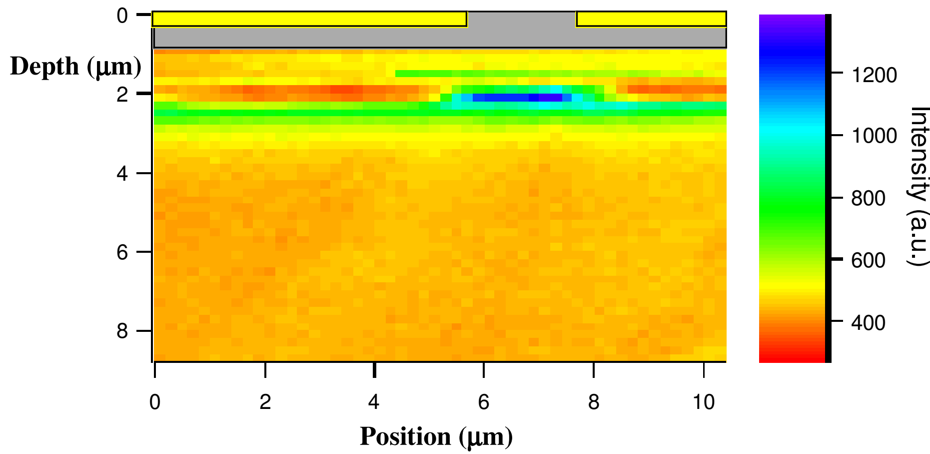

Experiment 1

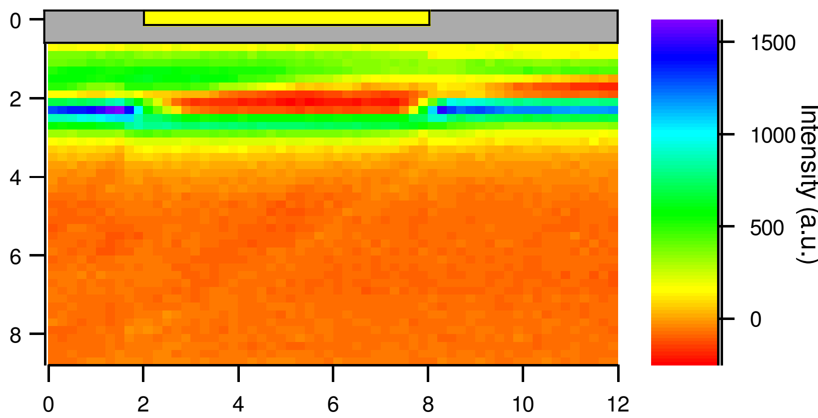

Experiment 2

Figure 4.12: *Raman intensity measured near structure 3, experiment 1 and 2. Top drawings indicate the position of the trenches (yellow) and the active regions (grey). In experiment 2, the 2 µm active region is located at the left. Left axis: depth, bottom axis: position.*

Figure 4.13 shows the corresponding Raman shift measured for both experiments.

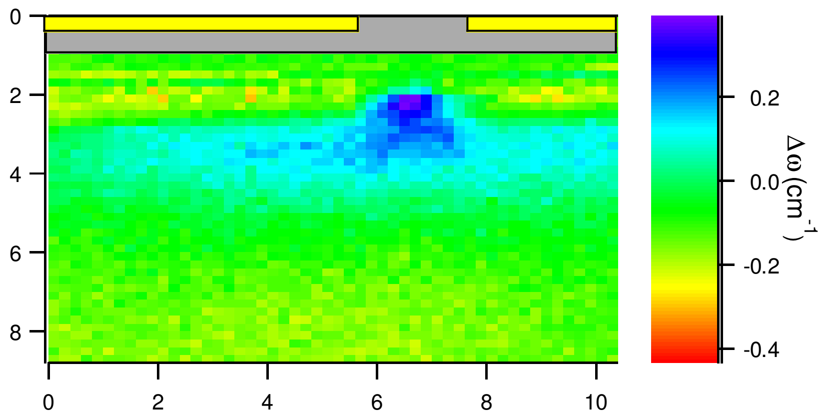

Experiment 1

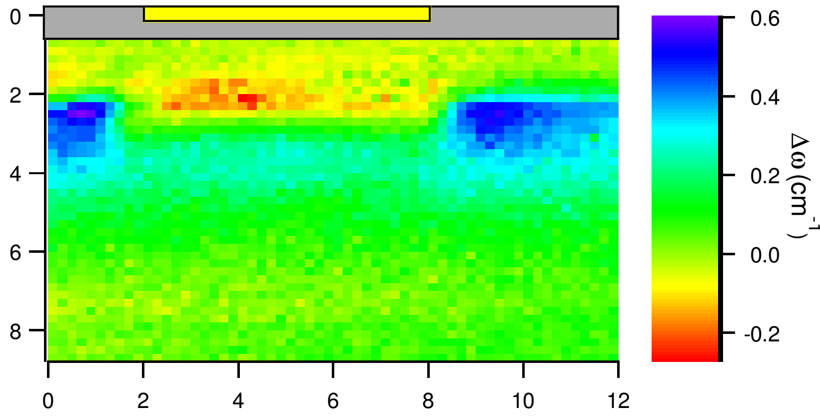

Experiment 2

Figure 4.13: *Raman frequency shift measured near structure 3, experiment 1 and 2. Top drawings indicate the position of the trenches (yellow) and the active regions (grey). In experiment 2, the 2 µm active region is located at the left. Left axis: depth, bottom axis: position.*

In both figures, we clearly see a positive Raman shift in the active region, indicating compressive stress. In order to have a better comparison (the figures have a different scale), both figures are shown together in Figure 4.14, using the same scale. As zero stress value, the value at the bottom of the graph was taken.

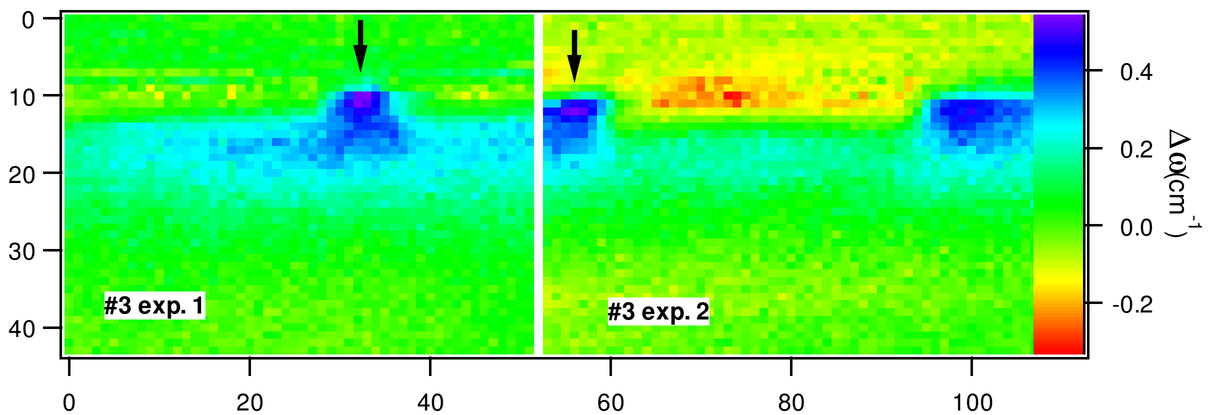

Figure 4.14: *Raman frequency shift measured near structure 3, experiment 1 and 2. The same scale is used for the colour code. The zero-stress value is taken at the bottom of the curves (depth 8.8 µm). The arrows indicate the position of the 2 µm wide active region. Left axis: depth, bottom axis: position.*

The two experiments give the same results. Figure 4.15 shows experiment 1 in a 3-Dim surface plot. The bottom axes in this plot indicate the position on the sample (depth and position (parallel to wafer surface)), not in µm but in point number. The vertical axis indicates the Raman frequency shift. Here one can clearly see the local increase in the Raman shift at the active region (blue top, up to 0.5 cm^{-1}), and the slow decrease of the Raman shift with distance from the surface (the bottom is at the left side in the graphs, the surface near x point nr. 10). The axis in this plot are in point number, the distance between 2 points is 0.2 µm. It is clear that the Raman shift decreases up to a distance of about 20 to 30 points, i.e 4 to 6 µm from the surface. This indicates that the stress from the surface extends deep into the silicon. This finding should be compared to findings from the finite element simulations.

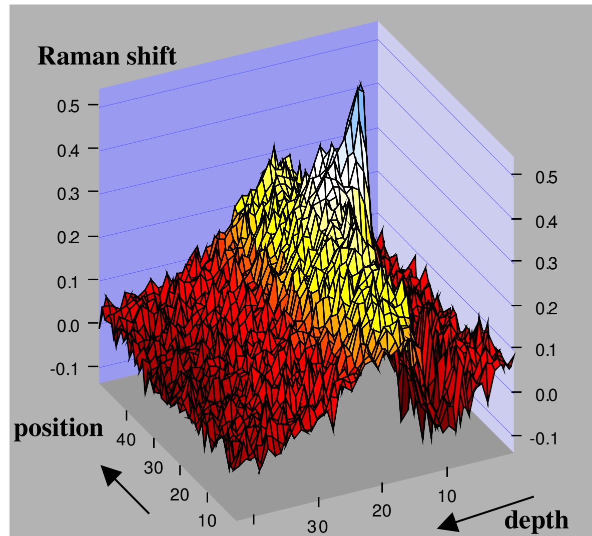

Figure 4.15: *Surface plot of the Raman frequency shift near structure 3, experiment 1. The zero-stress value is taken at the bottom of the sample (deep in substrate, position ~40 in these curves). The position and depth axes are in 'point number'. The distance between two points is 0.2 µm.*

4.1.3.2 Structure 2

Figure 4.16 shows the Raman intensity measured in two different experiments on structure 2.

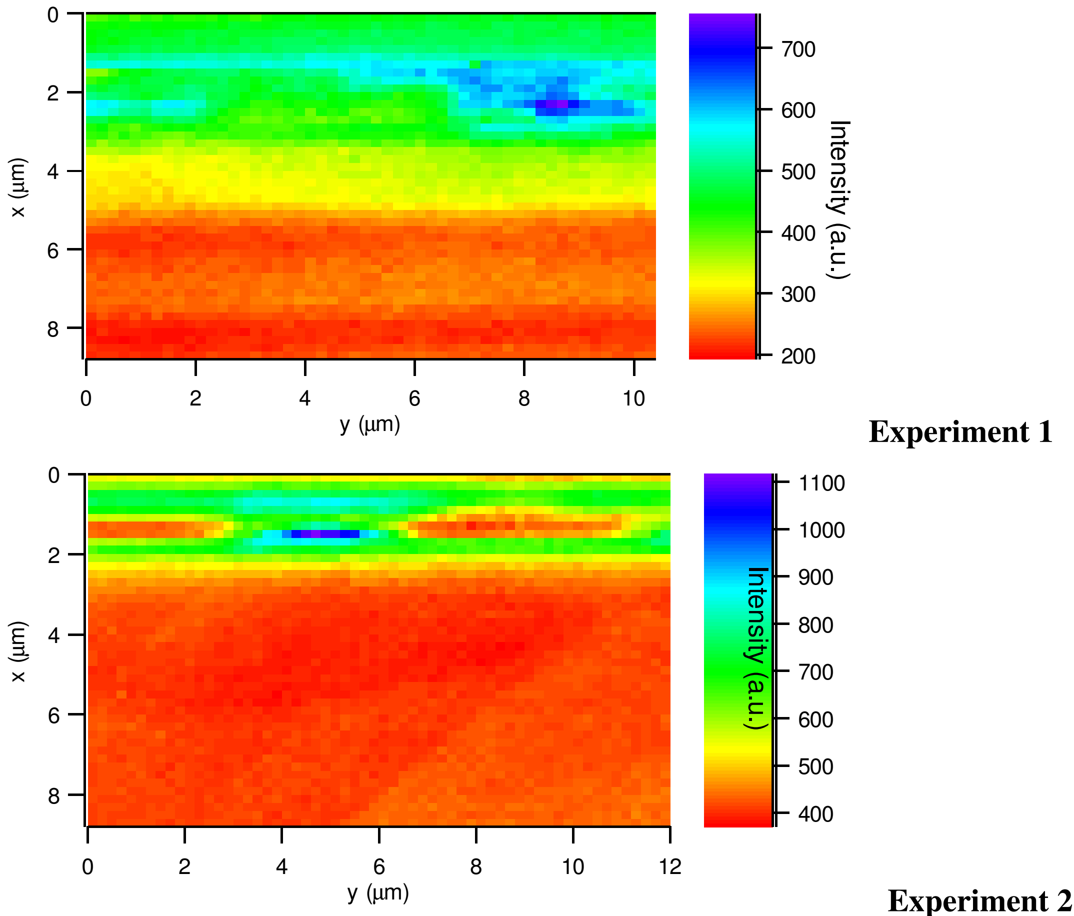

Figure 4.16*: Raman intensity measured near structure 2, experiment 1 and 2. Left axis: depth, bottom axis: position.*

Figure 4.17 compares the Raman shifts measured in these structures. The same scale is used as in figure 4.14. The position of the 2 µm wide trench was not really clear in experiment 1. For that reason, we will use only experiment 2 for further discussions.

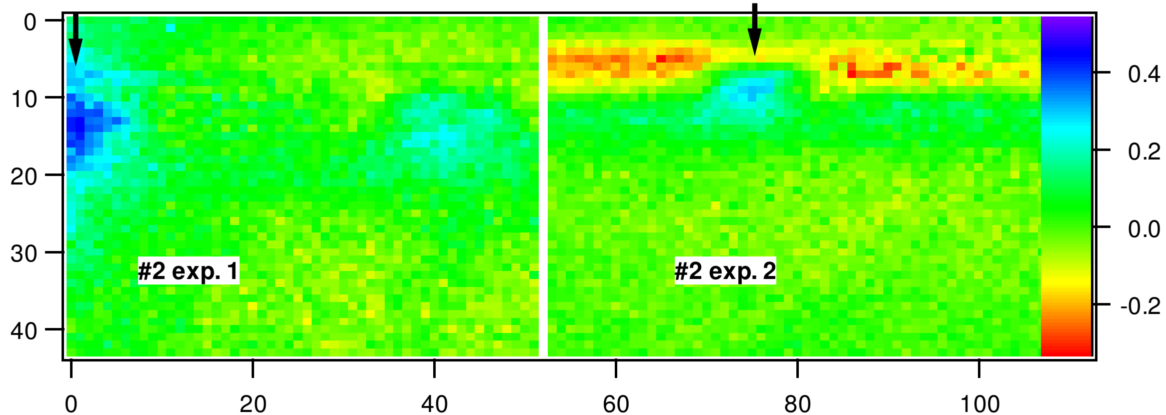

Figure 4.17: *Raman frequency shift near structure 2, experiment 1 and 2. The same scale is used for the color code. The zero-stress value is taken at the bottom of the curves. The arrows indicate the position of the 2 µm wide active region, however, for experiment 1 it is not clear where this position is. It might as well be the light blue spot at the right. Left axis: depth, bottom axis: position.*

Figure 4.18 shows experiment 2 in 3D plots. Here one can also clearly see the local increase in the Raman shift at the active region (blue top, up to 0.3 cm^{-1}), but the decrease of the Raman shift with distance from the surface seems to be steeper than for structure 3 (the bottom is at the left side in the graphs, the surface near x point nr.10). The axis in this plot are in point number, the distance between 2 points is 0.2 µm. It seems even that a small region of tensile stress is reached near point 30. The Raman shifts decreases up to a distance of about 10 to 15 points from the surface here, i.e 2 to 3 µm from the surface.

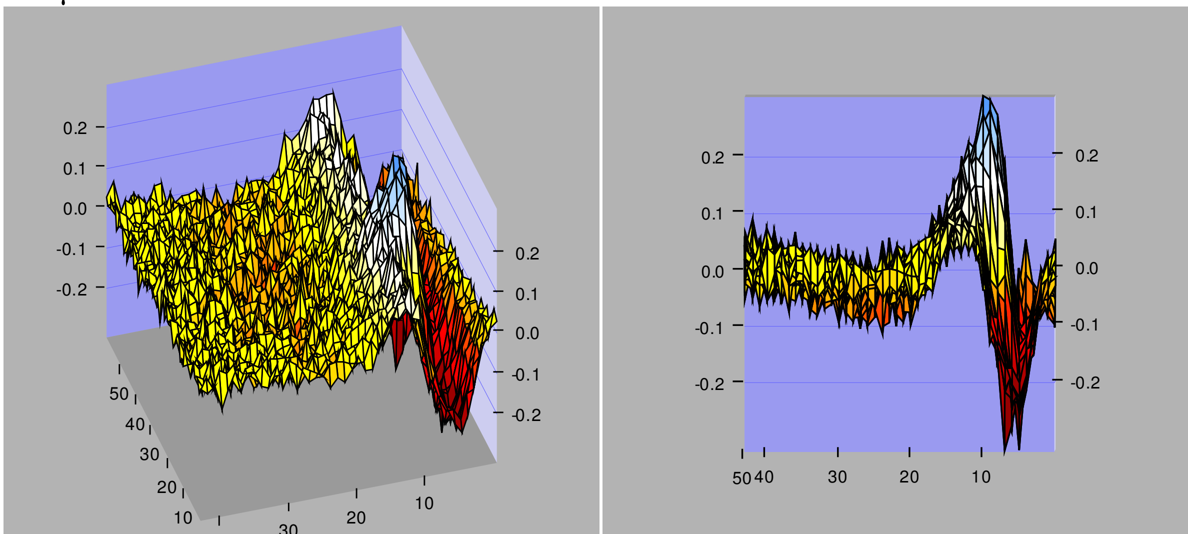

Figure 4.18: *Surface plot of the Raman frequency shift measured near structure 2, experiment 2. The axes are similar to the ones from Fig. 4.15. The zero-stress value is taken at the bottom of the sample (deep in substrate, position ~40 (@ depth 8 µm) in these curves). The horizontal axes are in 'point number'. The distance between two points is 0.2 µm. The figure at the right shows a 'side' view of the figure at the left, the bottom axes is the depth.*

4.1.3.3 Structure 1

Figure 4.19 shows the Raman intensity measured in two different experiments on structure 1. The bright blue region at the right side in Exp. 1 and left from the center in Exp. 2 indicates the position of the 2 µm wide active region.

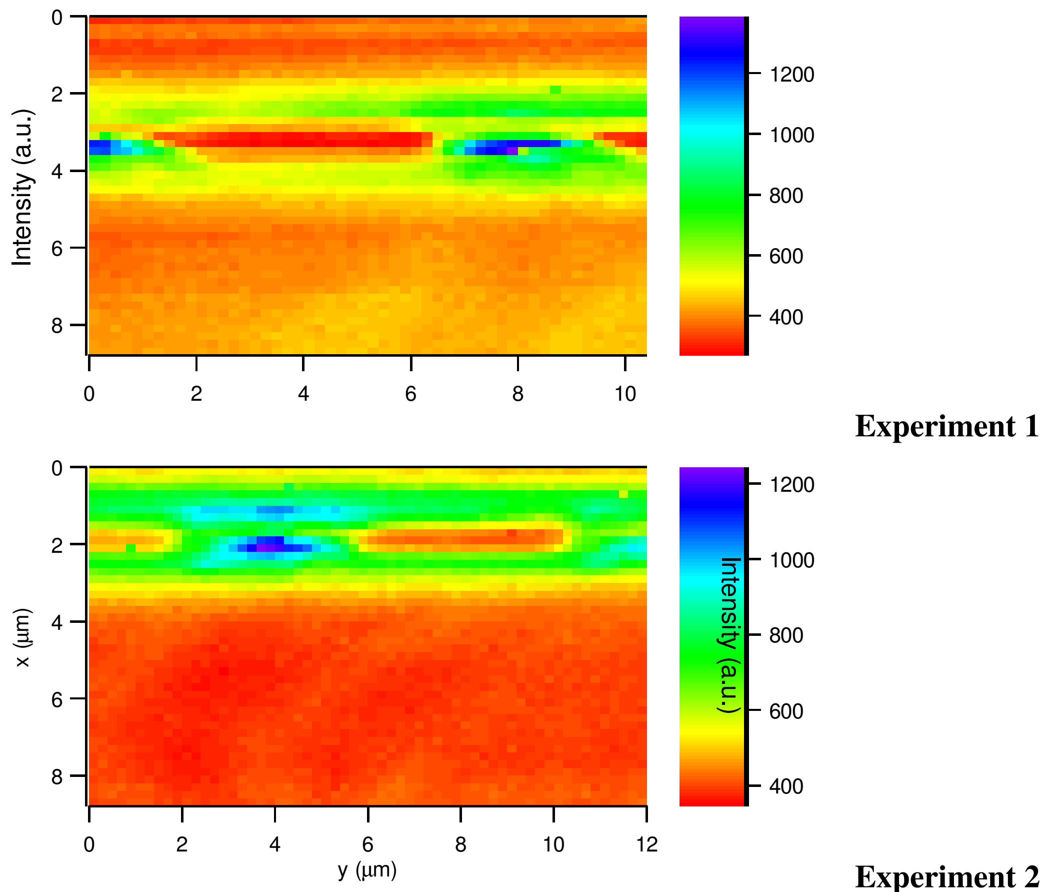

Figure 4.19: *Raman intensity measured near structure 1, experiment 1 and 2. Left axis: depth, bottom axis: position.*

Figure 4.20 compares the Raman shift for these two experiments. Again the same scale is used as in the similar figures from structure 3 and 2.

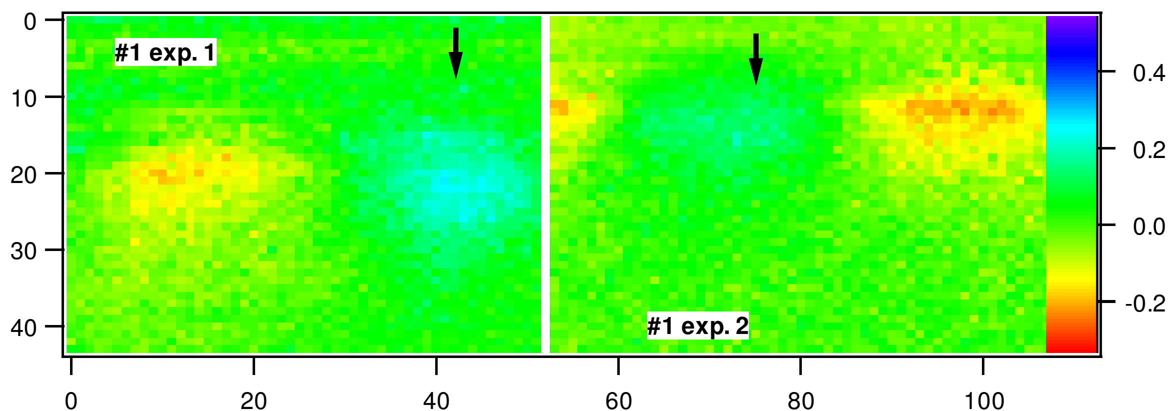

Figure 4.20*: Raman frequency shift measured near structure 1, experiment 1 and 2. The same scale is used for the colour code. The zero-stress value is taken at the bottom of the curves (@ depth ~8 µm). The arrows indicate the position of the 2 µm wide active region. Left axis: depth, bottom axis: position.*

Again we detect compressive stress in the active region, however, it is clearly much lower than for structure 3. Figure 4.21 shows surface plots for experiment 2 of this sample. The left figure is looked at from the surface side to indicate the compressive region (light blue, up to about 0.2 cm^{-1}) in the active area and the tensile regions (red) under the trenches. These tensile regions were also present in the other structures.

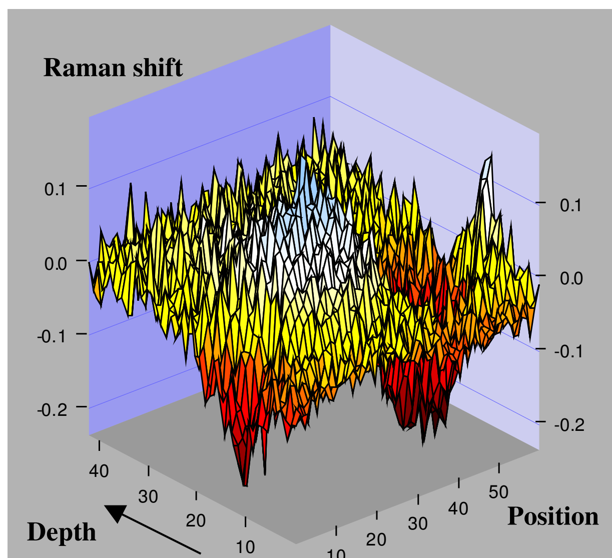

Figure 4.21: *Surface plot of the Raman frequency shift measured near structure 1, experiment 2. The zero-stress value is taken at the bottom of the sample (deep in substrate, (@ depth ~8 μm, position ~40 in these curves). The horizontal axes are in 'point number'. The distance between two points is 0.2 μm. The view point is in this figure from the 'surface' of the sample.*

4.1.3.4 Comparison of structures 1, 2 and 3.

Figure 4.22 compares the best experiments from the three positions. One can clearly see that the compressive stress in the active region decreases with decreasing distance to the hole in the sample. All figures had as reference the bottom side (zero stress value). This might not be entirely correct, but it clearly shows a decreasing trend in the stress. In the line scan, only for structure 1 a decrease in stress was observed.

Furthermore, while the stress in clearly concentrated in a small region in structures 3 and 2, it seems to be wider distributed in structure 1. This fits with what was observed in the line-scan experiment.

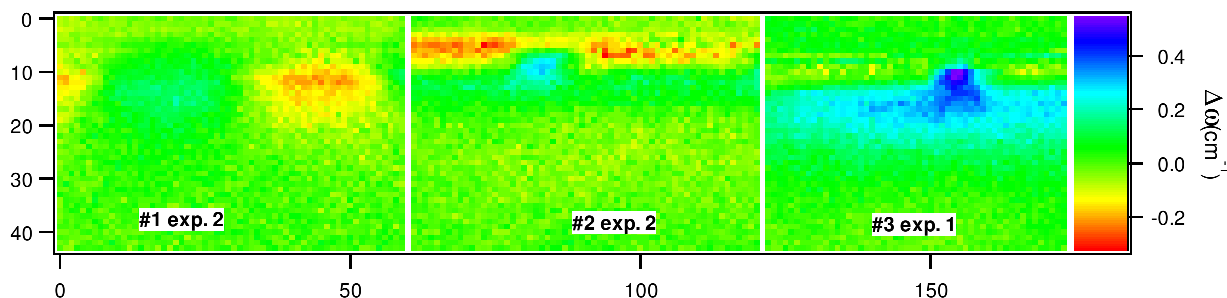

Figure 4.22: *Raman frequency shift measured near structure 1 (exp. 2), 2 (exp. 2) and 3 (exp1). The same scale is used for the colour code. The zero-stress value is taken at the bottom of the curves (@ depth 8 μm).*

Figure 4.23 shows surface plots (the two plots, a and b, are the same, but seen from a different viewpoint) of the three structures on the same graph. The data were somewhat smoothed for clarity. The absolute 'position' number is not correct, the distance between the structures is larger. But they are put together for comparison. It is clear here that when we take the Raman shift at the maximal depth (8.8 µm) as reference, structure 3 seems to have higher stress than structure 2 and structure 2 is again higher than structure 1.

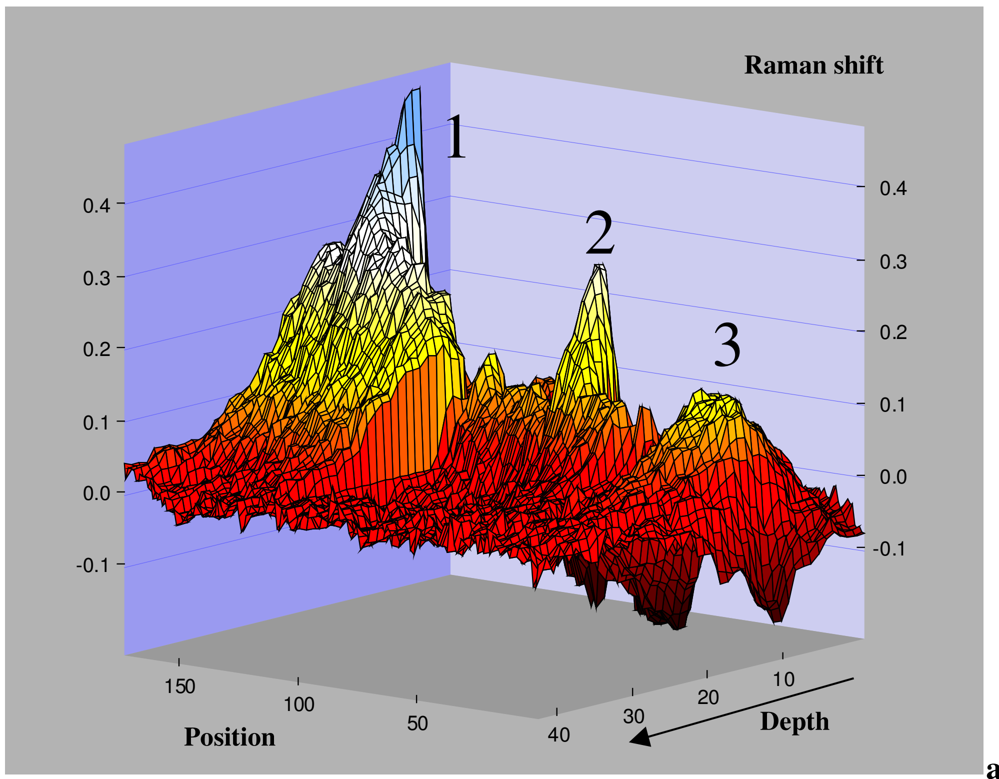

a

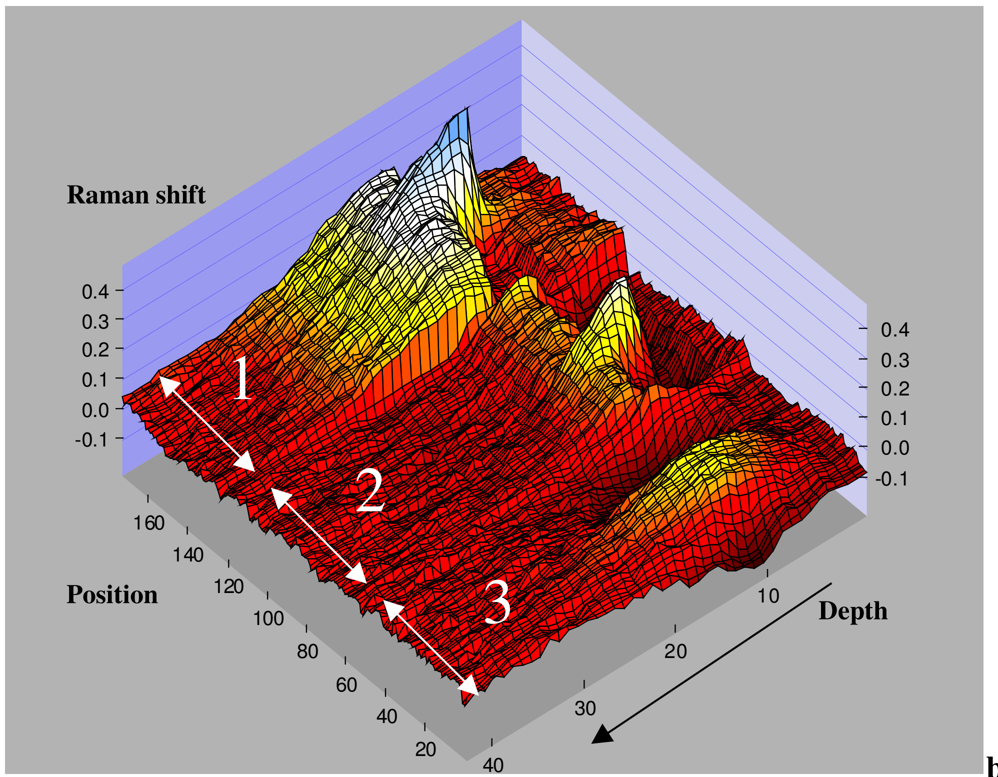

Figure 4.23: ***a)*** *Surface plot of the Raman frequency shift measured near structure 1 (exp. 2), 2 (exp. 2) and 3 (exp1). The same scale is used for the colour code. The zero-stress value is taken at the bottom of the curves (@ depth 8 μm).* ***b)*** *Same graph but from a different viewpoint.*

However, if we would take the Raman shift under the trench region as reference, as we did in the experiments from the top (Fig. 4.9) this difference is smaller. This can be seen in Fig. 4.24.

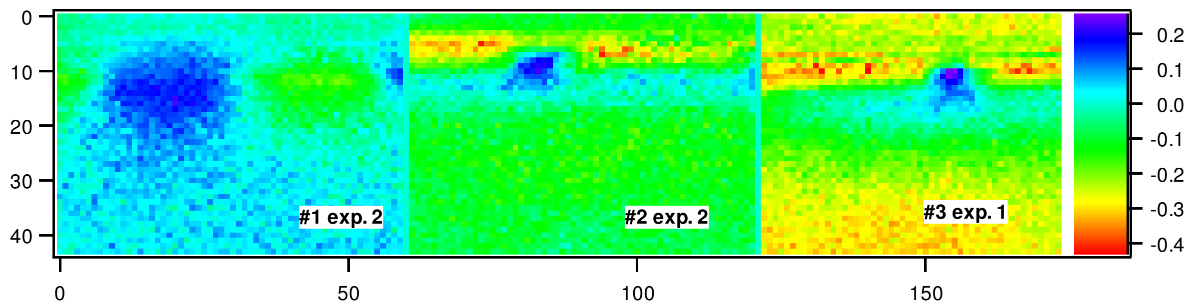

Figure 4.24: *Raman frequency shift measured near structure 1 (exp. 2), 2 (exp. 2) and 3 (exp1). The same scale is used for the colour code. The zero-stress value is taken at the bottom of trenches next to the active region.*

This might explain why we did not see a large difference between structure 2 and 3 when measuring from the top surface: the zero-stress reference was taken under the large trenches and not at a position far under the surface.

4.1.3.5 Conclusions TEM sample measurements

We showed that as well 1 dimensional as 2 dimensional Raman experiments can be performed on cross-sectioned samples, prepared for TEM analysis.
There are clearly effects of the sample thinning on the Raman results:

- there is influence on the Raman intensity as soon as the sample becomes thinner than the probing depth of the laser used for the experiments. This can be used to determine the sample thickness, but has no further effect on the results
- there is clearly a heating effect as soon as the sample becomes thinner than 2.6 µm. The heating of structure 1 is about 12 °C. There is no difference in heating between structure 2 and 3. CBED experiments are typically performed at positions where the silicon is even thinner than structure 1, i.e. about 0.3 µm thick, and the heating is about 20 °C.

The line scan indicates stress relaxation and a broader stress distribution in structure 1 which is located at about 34 µm from the hole, sample thickness 0.9 µm.

It is found that the relation between the Raman shift and the stress tensor components is different when measuring from the top of the sample and from the side. This could help to give more detailed information on the separate stress tensor elements, and compare the results with simulations.

The two-dimensional scans show compressive stress in the 2 µm structure. The interpretation of the results is difficult because we do not have a good stress-free reference and we have to correct for temperature effects (heating). For the latter we assume that the temperature increase of 12 °C near structure 1 did not affect the local stress distribution, i.e. is the same over the whole experiment near structure 1.

- the experiments indicate that the compressive stress decreases with decreasing distance to the hole, i.e. with increasing thinning of the sample (3->2->1). This stress decrease might be due to a stress relaxation due to thinning of the sample. Because the difference in heating between 2 and 3 was found to be very small, the difference in stress between these structures is probably not due to heating. On the other side, we did not see a difference between 2 and 3 when doing the line scan.
- There is clearly a large stress reduction (both in the line scan and in the 2D scans) in structure 1. This might indicate stress relaxation. However, we cannot completely rule out that there are also temperature effects due to the heating by the Raman laser.

It is clear from these experiments that Raman spectroscopy provides very interesting information on stresses in the samples. However, there are still questions to be resolved. The most important one is whether the stress reduction observed in the TEM sample is due to local heating of the sample by the laser or to sample thinning induced stress relaxation. More experiments have to be performed to resolve this issue. Also numerical simulations could help to resolve this issue. The following actions are planned:

- Simulations of Raman shift measured from the top of a sample and from the side
- Further calculations to compare Raman experiments from a (100) surface with experiments from a (110) surface.
- Measurement on TEM sample with a high density of similar structures (if possible with silicide, to compare at the same time the stress with and without silicide), for examples space – active arrays of 3 µm, to see whether this stress relaxation effect starts together with the heating effect.
- Comparison with numerical simulations: effect heating to 12 °C on the local stress, etc.

5. Comparison with analytical models

A direct comparison of the Raman results with analytical models was not performed yet. Figure 5.1 shows the result of an analytical model describing stress imposed by an 'inclusion' in the silicon [4]. The inclusion being the trench. The model assumes that the trench is infinitely long, so that plane strain can be assumed. A macro was written in the program 'IGOR Pro' (WaveMetrics Inc., a program which we also use to fit the Raman data) to calculate the stress components following this model. First results using this macro are shown in Fig. 5.1. The model was adapted so that instead of the result of only one inclusion (as shown at the top of Fig. 5.1), also the effect of two inclusions (i.e. a trench at the left side and the right side of the active region) could be calculated. This is shown at the bottom of Fig. 5.1. The data are at the moment not calibrated. We still have to include material parameters of the oxide and the silicon. However, the first results look promising: they indicate compressive stress in the top of the trench and tensile near the side walls.

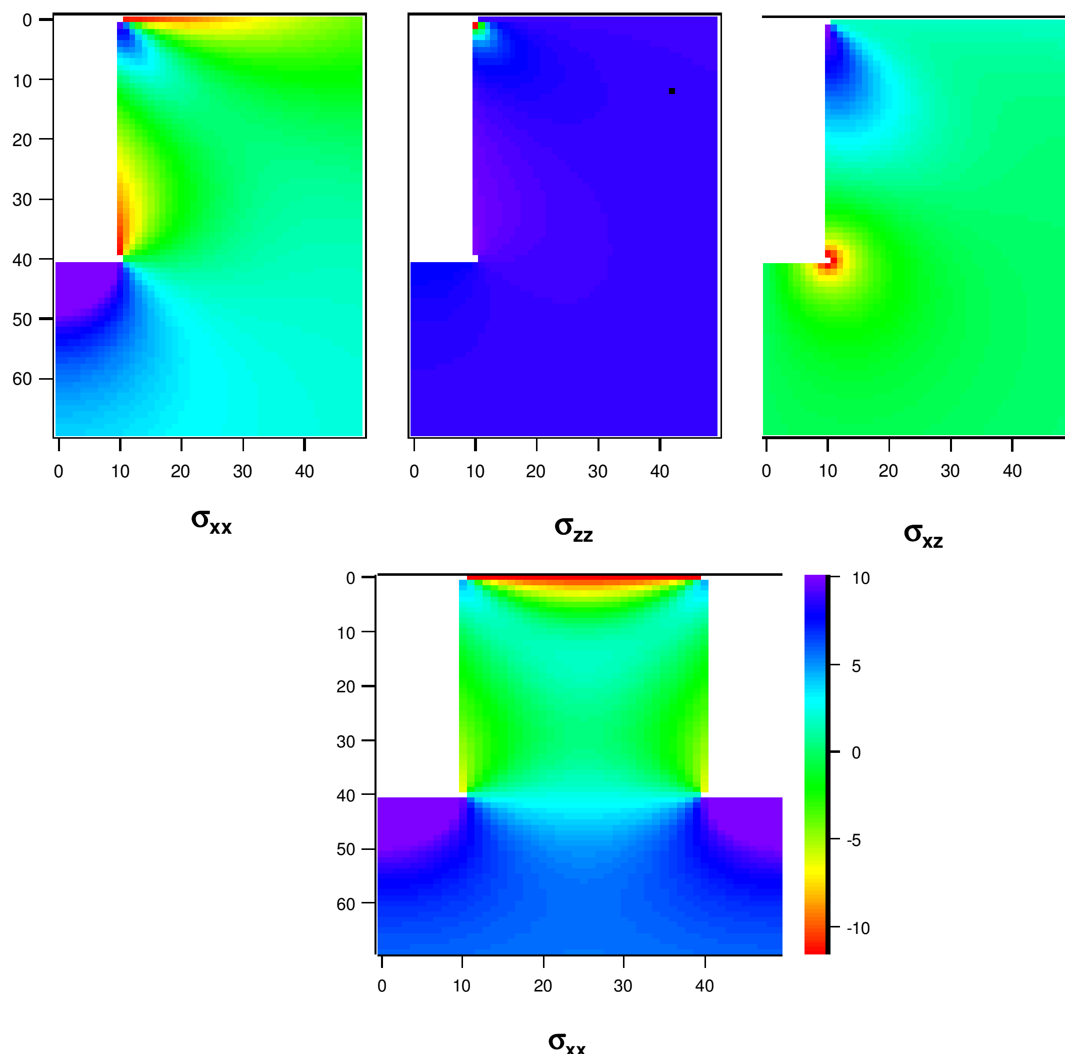

Figure 5.1: *First results from the analytical model of trenches.*

In the following steps, a nitride layer will be added to this model. Next this model will be applied to structure V004808_20 and compared with the 1D and 2D Raman data described above, with the numerical models from this structure (see report IST10341-IS-RP004) and if possible with the XRD data.

6. Comparison with numerical models

The comparison of Raman data from samples from the first campaign with numerical data was reported already in deliverable D12A (IST10341-IS-RP004). In general a very good agreement between Raman data and simulations was obtained, especially in the active region.

The agreement was only bad for sample 14 (see Fig. 21b in IST10341-IS-RP004). However, as discussed above (Figs. 2.2 and 2.3 in this report), that was due to a measurement error in the Raman experiment. The data from a new experiment give a much better fit with the model.

A comparison of data from the second measurement campaign with the numerical model was not possible because we could not measure stress under the silicide. Experiments are planned on a TEM prepared sample in cross-section to obtain some Raman data which can be used for this purpose.

We also hope that by using Raman data obtained from the surface as well as from the interface, we can provide more information on the different stress tensors to the numerical models. However, one has to keep in mind that Raman has a limited spatial resolution, even in cross section measurements the size of the probing laser spot is still larger than the depth of the trenches.

7. Comparison with CBED

The comparison of Raman and CBED data was reported in detail in Deliverable D8 and Deliverable D12a.

It was shown that a direct comparison was difficult because of the large spot size of Raman, and, especially the large penetration depth. The latter is not so important when measuring in cross-section. Indeed, in cross section the depth of analysis with micro-Raman spectroscopy and CBED are about the same, i.e. 0.3 µm. So, the above discussed cross-section experiments are better for comparison with CBED data. However, more Raman experiments should be performed first to find out the exact influence of sample thinning and laser heating on the local stress in such samples. It seems that Raman experiments should be performed on samples thicker than 2.5 µm to avoid sample heating, while CBED experiments are limited to samples thinner than 0.3 µm, due to inelastic scattering (which increases with thickness).

8. General conclusions

In this report, we concentrated on a discussion of the 2-Dim Raman measurements on a TEM cross-section sample.

Further, we referred to existing deliverables and intermediate reports where Raman results and comparison with CBED and numerical simulations were reported in detail.

In general, it is clear that Raman spectroscopy can provide valuable information on local stress developed during a process. The technique does not require sample preparation and offers rather fast information. When compared to CBED, it is faster and simpler. However, it is clear that its major drawback compared to CBED is the large spot size, i.e. the limited spatial resolution. This

drawback becomes more and more important with the increasing densification and miniaturisation of devices. It is clear that Raman, in the present state of the art, is only useful for dimensions equal to or larger than 2 µm.

It is possible to improve the spatial resolution of the technique through means of SIL lenses or special objectives, such as oil or water immersion objectives. Experiments performed during the STREAM project with SIL lenses were rather negative. Experiments with an oil immersion objective were very promising, but gave the problem that the oil started burning during the experiment, because of the heating by the laser. A water immersion objective, although it would not give as good a resolution as an oil immersion objective, would be a solution, but could not be tested because it was not available. Another kind of oil could maybe solve the problem, but it was outside the scope of this project to test this. The problem of the oil was reported to the Raman instrument vendor ISA Jobin-Yvon (Lille, France; previously named DILOR) and the oil immersion lens was passed to them for some further tests.

The Raman data did correspond very well to the numerical calculations. Some more work is planned to compare the 2-D data.

A direct comparison between Raman data and CBED turned out to be difficult because of the difference in spatial resolution. It is better to compare both techniques through the numerical simulations, as was shown in Deliverable 12A.

References

1. Anastassakis E. and Burstein E. J. Phys. Chem. Solids 1971; 32: 563-570.
2. Anastassakis E., Canterero A. and Cardona M.. Phys. Rev. B 190; 41(11): 7529-7535.
3. De Wolf I. Topical Review: Micro-Raman spectroscopy to study local mechanical stress in silicon integrated circuits. Semicond. Sci. Technol. 1996; 11: 19
4. De Wolf I., Stress measurements in Si microelectronics devices using Raman spectroscopy, J. Raman spectrosc. 1999; 30:877-883.
5. Raman and Luminescence Spectroscopy for Microelectronics. Catalogue of optical and physical parameters. EC Nostradamus project SMT4-CT-95-2024, EUR 18595. Editors: I. De Wolf, J. Jimenez, J-P Landesman, C. Frigeri, P. Braun, E. Da Silva, E. Calvet.
6. M. van Spengen, I. De Wolf, R. Knechtel. Experimental one and two-dimensional mechanical stress characterization of silicon microsystems using micro-Raman spectroscopy. Proc. of SPIE Vol. 4175, pp. 132-139, 2000
7. General report from Nostradamus project EC, SMT4-CT-95-2024
8. S.M. Hu. Stress from a parallelepipedic thermal inclusion in a semispace. J. Apl. Phys. 66(6), pp. 2741-2743, 1989.